HHS Public Access

Author manuscript

Hepatol Res. Author manuscript; available in PMC 2015 September 01.

Published in final edited form as:

Hepatol Res. 2015 July ; 45(7): 794–803. doi:10.1111/hepr.12411.

Inhibition of the CXCL12/CXCR4 chemokine axis with AMD3100, a CXCR4 small molecule inhibitor, worsens murine hepatic injury

Yedidya Saiman[1], **JingJing Jiao**[1,*], **M. Isabel Fiel**[1], **Scott L. Friedman**[1], **Costica Aloman**[1,†], and **Meena B. Bansal**[1]

[1]Division of Liver Diseases, Department of Medicine, Icahn School of Medicine at Mount Sinai, New York, NY.

Abstract

Aim—Activation of hepatic stellate cells and development of chronic inflammation are two key features in the progression of hepatic fibrosis. We have shown that *in vitro* activated stellate cells increase their expression of CXCL12 as well as the receptor CXCR4 and that receptor engagement promotes a profibrogenic phenotype. Furthermore, injury promotes increased hepatic expression of CXCL12 and a massive infiltration of CXCR4-expressing leukocytes, granulocytes, and myeloid cells. The primary site of inflammatory cell accumulation is around the CXCL12-rich portal tracts and within fibrotic septae, indicating a role for CXCR4 during injury. In order to characterize the relevance of the CXCR4/CXCL12 chemokine axis during hepatic injury we inhibited the axis using AMD3100, a CXCR4 small molecule inhibitor, in models of chronic and acute liver injury.

Methods—Mice were subjected to acute and chronic CCl_4 liver injury with and without AMD3100 administration. The degree of liver injury, fibrosis, and the composition of the intrahepatic inflammatory response were characterized.

Results—Treatment of mice with AMD3100 in the chronic CCl_4 model of liver injury led to an increase in hepatic inflammation and fibrosis with a specific increase in intrahepatic neutrophils. Furthermore, in an acute model of CCl_4 induced liver injury, AMD3100 led to an increase in the number of intrahepatic neutrophils and a trend towards worse necrosis.

Conclusions—Together, this data suggests that inhibition of the CXCR4/CXCL12 chemokine axis is injurious through modulation of the hepatic inflammatory response and that this axis may serve a protective role in liver injury.

Keywords

CXCR4; CXCL12; Hepatic Stellate Cells; Liver Fibrosis

Corresponding Author: Meena B. Bansal, M.D. Icahn School of Medicine at Mount Sinai 1425 Madison Avenue, Room 11-70 Box 1123 New York, NY 10029 meena.bansal@mssm.edu Fax: 212-849-2574.

*Present Address: Department of Molecular and Cellular Oncology, The University of Texas MD Anderson Cancer Center, Houston, TX.

†Present Address: Division of Gastroenterology and Hepatology, Department of Medicine, University of Illinois College of Medicine at Chicago, Chicago, IL.

No conflicts of interest, financial or otherwise are declared by the authors.

Introduction

Chemokines are small molecular weight proteins (8-13 kD) initially identified by their ability to provide migratory cues to inflammatory cells [1]. Their expression is up-regulated in nearly all forms of tissue injury promoting immune cell infiltration and activation. The contribution of chemokines to the progression of liver disease is well established. Mice deficient in chemokine receptors CCR1, CCR5 [2], CCR2 [3, 4], and CCR7 [5], demonstrate a decrease in the extent of injury in both chronic fibrotic and acute necrotic liver injury. Alternatively, some chemokine axes appear to be protective and their loss leads to worse outcomes in models of liver disease [6, 7].

Knowledge about the specific role of CXCL12 in chronic inflammatory and fibrotic diseases is fragmentary. Together with its primary receptor, CXCR4, the CXCL12 axis plays a major role in immune and hematopoietic cell egress and mobilization during homeostatic and injury conditions. CXCL12 levels are increased in many diseases including: pulmonary fibrosis [8], systemic lupus erythematosus [9], rheumatoid arthritis [10], multiple sclerosis [11], and inflammatory bowel disease [12]. In these diseases, CXCL12 recruits subtypes of inflammatory cells that are injurious. Specifically, in pulmonary fibrosis, inhibition of the CXCL12/CXCR4 axis with either a CXCL12 neutralizing antibody, or AMD3100, a CXCR4 small molecule inhibitor, leads to a decrease in the number of bone marrow-derived fibrocytes, and overall better outcome [8]. Additionally, administration of AMD3100 in certain models of myocardial infarction decreased the extent of tissue scarring and improved cardiac function [13, 14]. Given these findings, the potential therapeutic benefit of AMD3100 has been discussed[15].

CXCL12 expression has been detected both in the normal and injured liver though its function remains largely unknown. It is expressed by biliary epithelial cells [16], hepatic stellate cells [17], and hepatic sinusoidal endothelial cells [18]. In patients with liver disease, CXCL12 protein levels are increased in both the liver and plasma and correlate with the extent of fibrosis [16]. With hepatic injury there is an infiltration of CXCR4-expressing immune cells including lymphocytes, granulocytes, and monocytes primarily around the CXCL12-rich periportal regions, indicating the importance of this axis. The function of each of these cell populations is only now being uncovered, but they already show competing roles in fibrosis and its resolution [19-22].

Activation of hepatic stellate cells (HSCs) and development of chronic inflammation are two key features driving the progression of hepatic fibrosis. We have shown that *in vitro*, HSC activation drives expression of both CXCL12 and its receptor CXCR4 and that recombinant CXCL12 promotes a pro-fibrogenic phenotype [17]. Therefore, hepatic CXCL12 may play multiple roles during injury by recruiting inflammatory cells and driving stellate cell activation. In this study we use AMD3100, a well-established small molecule inhibitor of CXCR4 to study the role of the CXCL12/CXCR4 axis in chronic fibrotic and acute necrotic models of liver injury.

Methods

Mouse Models of Fibrosis

All experiments were performed on C57Bl/6 male mice purchased from NCI (Bethesda Maryland). For induction of fibrosis using the chronic CCl_4 model mice received 100μL of 10% CCl_4 diluted in corn oil 3X a week for four weeks. Mice were sacrificed 48 hours after the last injection. Acute liver injury was induced by a single injection of 100μL of 25% CCl_4 diluted in corn oil and sacrificed as indicated. This study was carried out in strict accordance with the recommendations in the Guide for the Care and Use of Laboratory Animals of the National Institutes of Health. The protocol was approved by the Institutional Animal Care and Use Committee (IACUC) of the Mount Sinai School of Medicine (Permit Numbers: LA10-00059 and SP10-00363).

Administration of AMD3100

AMD3100 was administered either by continuous subcutaneous infusion with an osmotic pump (Alzet Osmotic Pumps) or by once weekly by I.P. injection. Osmotic pumps, which deliver 0.11μL/hr, were loaded with 100μL of 83.3mg/mL AMD3100 in PBS. Mice were anesthetized and a small incision and pocket made on the dorsal side. The pump was inserted and the incision closed with a staple. The total daily dose of AMD3100 administered over 24 hours was 200μg. For I.P. injections, mice received 200μg of AMD3100 in 100μL PBS. Mice that received a single dose of CCl_4 for acute liver injury were additionally treated with or without a single injection of 100μg AMD3100 12 hours after CCl_4 administration.

Analysis of liver function enzymes

Peripheral blood was collected via retro-orbital bleeding and immediately mixed with 0.5mM EDTA to prevent coagulation. 500μL blood was transferred into a Microtainer Plasma Separator (BD, Franklin Lakes, NJ), centrifuged according to manufactures recommendations and plasma stored at −80°C until analysis. Analysis was performed at the Mount Sinai Medical Center Clinical Laboratory.

Histological scoring

At time of sacrifice mouse livers were perfused with 10mL PBS and half the right lobe harvested and fixed in 10% formalin for 24hr and embedded in paraffin. Histological scoring of murine livers was performed by an expert hepatobilliary pathologist. All parameters are scored on a scale of 0-4. For each mouse, 10 high power fields were assessed.

Sirius red staining

Five-micron sections were stained for collagen with Sirius red (0.1% solution, diluted in picric acid, both from Sigma, St. Louis, MO). Percent fibrosis was assessed based on 36 10X-fields from Sirius red stained liver sections per animal in a blinded fashion. Each field was analyzed using a computerized Bioquant® morphometric system. Overall fibrosis was assessed by intensity of Sirius red staining.

Immunohistochemistry

Formalin-fixed, paraffin-embedded liver tissue obtained mice were deparaffinized, rehydrated, incubated with DAKO (Carpinteria, CA) Peroxidase block for 5 minutes followed by incubation with DAKO Serum Free Protein Block at room temperature for 10 minutes. Rabbit polyclonal anti-α smooth muscle actin antibody (Abcam, Cambridge, MA, catalog #ab-56984) at a dilution of 1:500 was used for overnight incubation at 4°C. Both primary isotype control antibody and secondary antibody with no primary antibody were used as negative controls. Slides were washed three times and revealed using DAKO Envision Plus System. Nuclei were stained with hematoxylin and percent α-SMA staining was assessed based on 25 100X-fields per animal in a blinded fashion. Each field was analyzed using a computerized Bioquant® morphometric system.

RNA isolation and quantitative real-time PCR

Murine livers were collected and stored in RNAlater (Qiagen, Valencia, CA) until time of use. RNA was isolated by homogenization and purification in TRIzol reagent (Invitrogen, Grand Island, NY) followed by RNAeasy clean-up with on-column DNA digestion (Qiagen). Reverse transcription was performed using RNA to cDNA EcoDry Premix Double Primed Kit (Clontech, Mountain View, CA) and quantitative real-time PCR performed using iScriptTM One-Step RT-PCR Kit with SYBR® Green (Bio-Rad, Hercules, CA). Quantification was performed by normalizing each Ct value to GAPDH and comparing ΔCt values between groups. Values are expressed either as absolute ΔCt or fold increase of experimental to control group. Primer sequences in Table 1.

Peripheral blood and liver leukocyte flow cytometry

Peripheral blood was collected via retro-orbital bleeding and immediately mixed with 0.5mM EDTA to prevent coagulation. Red blood cells were lysed by 3 washes in RBC lysis buffer, filtered, and washed in PBS/FBS followed by staining with antibodies for FACS analysis. For liver infiltrating leukocyte isolation, at the time of sacrifice the livers were perfused with 10mL PBS through the portal vein, carefully removed, and gallbladder excised. A portion of the liver was cut, weighed, chopped into small pieces and incubated in 0.01% Collagenase type IV (Sigma) at 37°C for 25 minutes. Liver tissue was then passed through a 70μm cell strainer and washed twice with PBS/FBS. Cells were resuspended in a 40% Percoll (GE Healthcare) and loaded onto a 70%/40% Percoll gradient and centrifuged at 2400 RPM at 24°C for 25 minutes with no acceleration or brake. The top layer of hepatocytes was removed and the liver infiltrating leukocytes located at the interface collected and washed 2X in PBS/FBS and cells counted. The following antibodies were used: rat anti-mouse CD45-APC-Cy7, clone: 30-F11 (BD Pharmigen), rat anti-mouse Ly-6G-Alexa Fluor 488, clone: RB6-8C5 (eBiosciences), rat anti-mouse Ly-6G-PE, clone: 1A8 (BD Pharmigen), rat anti-mouse TER-119-Biotin, clone: TER-119 (eBiosciences), rat anti-mouse CD3-Biotin, clone: 145-2C11 (eBiosciences), rat anti-mouse CD45R-Biotin, clone: RA3-6B2 (eBiosciences), rat anti-mouse NKp46-eFluor 450, clone: 29A1.4 (eBiosciences), rat anti-mouse CD11b-PerCP-Cy5.5, clone: M1/70 (eBiosciences), rat anti-mouse CD11b-Biotin, clone: M1/70 (BD Pharmigen), rat anti-mouse CD45R-APC-eFluor780, clone: RA3-6B2 (eBiosciences), rat anti-mouse Sca-1-APC, clone: D7

(eBiosciences), rat anti-mouse c-Kit-PE-Cy7, clone: 2B8 (eBiosciences). Multiparameter analyses of stained cell suspensions were performed on an LSRII (BD) and analyzed with FlowJo software (Tree Star, Inc).

Statistics

All results are expressed as the mean ± standard deviation. Statistical significance was tested using an unpaired Student's t and $P < 0.05$ indicated a significant difference.

Results

Increased hepatic expression of CXCL12 and CXCR4 in murine models of liver fibrosis

To determine whether there is an increase in protein and mRNA expression of CXCR4 and CXCL12 during murine liver injury we performed quantitative RT-PCR and Western blot analysis. In mice that received chronic CCl_4 injections there was a 16-fold increase in CXCR4 transcript (Fig. 1A) and a substantial increase in CXCR4 (Fig. 1B) and CXCL12 (Fig. 1C) protein expression by Western blot. Despite the increase in CXCL12 protein, there was no change in the transcript levels (Fig. 1D). To determine if there are changes in the three known murine CXCL12 splice variants, we designed primers that could distinguish between them (Table 1). No changes were observed in any of the splice variants for CXCL12 in CCl_4 treated livers (Fig. 1E).

Continuous inhibition of the CXCL12/CXCR4 axis with AMD3100 leads to an increase in fibrosis and intrahepatic neutrophils in the chronic CCl_4 models of liver fibrosis

Inhibition of the CXCR4/CXCL12 axis has been shown to decrease the extent of fibrosis in mouse models of pulmonary fibrosis. We therefore determined whether AMD3100 would have a similar effect in hepatic fibrosis. In the chronic CCl_4 model, mice that received a continuous infusion of AMD3100 showed a significant increase in hepatic collagen content and fibrosis as measured by Sirius red staining (Figs. 2A & B). In accordance with the increased fibrosis, there was an increase in hepatic α-smooth muscle actin (α-SMA) staining by immunohistochemistry in the mice receiving CCl_4 and AMD3100 over CCl_4 alone (Figs. 2C & D), suggesting an increase in stellate cell activation. Similarly, transcript levels of collagen 1α1 (Fig. 2E) and α-SMA (Fig. 2F) were increased ~2 fold in the mice receiving AMD3100. Although not statistically significant a similar trend toward increased fibrosis was seen in the bile duct ligation model of hepatic fibrosis (data not shown).

As AMD3100 promotes immune cell egress from the bone marrow, we analyzed peripheral blood and intrahepatic inflammatory cells after AMD3100 administration. FACS analysis of the peripheral blood did not demonstrate a change in circulating leukocytes after administration of CCl_4 alone (Fig. 3A, column 1 vs. 2), however the expected increase in circulating leukocytes due to AMD3100 was observed both in the control (Fig. 3A, column 1 vs. 3, 5×10^6 vs. 12×10^6 leukocytes/mL) and CCl_4 treated groups (Fig. 3A, column 2 vs. 4, 6×10^6 vs. 13×10^6 leukocytes/mL), with the greatest changes seen in the neutrophil population (Fig. 3B).

Within the liver, no changes in inflammation were observed by liver histological analysis (data not shown); however, FACS analysis revealed a significant increase in the absolute number of CD45-positive liver infiltrating immune cells per gram of liver in mice receiving AMD3100; both in the oil treated (Fig. 3C, column 1 vs. 3, 1.4×10^6 vs. 2.4×10^6) and CCl_4 treated groups (Fig. 3C, column 2 vs. 4, 2.5×10^6 vs. 4×10^6) again with a specific increase in the total number neutrophils (Fig. 3D) similar to the peripheral blood.

Once weekly administration of AMD3100 does not lead to any changes in the chronic CCl_4 model of liver fibrosis

In models of myocardial ischemia administration of AMD3100 after injury leads to divergent outcomes depending on the dosing regimen [13, 14]. Chronic augmentation of the CXCR4 axis with AMD3100 leads to an increased area of infarction and an expanded scar area while a single dose of AMD3100 shortly after induction of injury leads to increased myocardial vascularity, reduced fibrosis, and an overall increase in cardiac function. The single AMD3100 injection increased circulating endothelial progenitor cells, thought to be important in the revascularization of the myocardium after injury [14].

We therefore hypothesized that a single weekly AMD3100 injection during chronic liver injury may be beneficial in hepatic regeneration by releasing bone marrow progenitor cells. Fibrosis was induced by either 3X-weekly CCl_4 administration with injection of AMD3100 once weekly 12 hours after the last CCl_4 injection. We saw no differences in either the extent of fibrosis (Figs. 4A & B) or in the absolute number of inflammatory cells within the liver (Fig. 4C).

AMD3100 is not protective in CCl_4 induced acute hepatic injury

Bone marrow progenitor cells have the unique ability to attenuate the extent of injury in scenarios of massive hepatic insult. While the mechanism has not been elucidated, in nearly all forms of injury, delivery of bone marrow cell populations after injury promotes hepatic regeneration [23]. Administration of G-CSF and AMD3100 after a sub-lethal dose of CCl_4 attenuates the extent of injury with a concomitant increase in circulating CD34+ bone marrow progenitor cells [24]. Given the rapid activity of AMD3100 and maximal bone marrow mobilization at 9 hours [25], as opposed to G-CSF which takes days to reach maximal mobilization [26], we tested whether AMD3100 alone could confer protection after administration of a sub-lethal CCl_4 dose. Mice received 25μL CCl_4 followed by 100μg AMD3100 12 hours later and were sacrificed between 36 and 144 hours after receiving CCl_4.

There were no significant differences in hepatic injury measured by ALT and AST (Figs. 5A & B); however, by histological analysis there was a trend towards an increased degree of necrosis at 36 hours in mice administered AMD3100 (Figs. 5C & D). While there was only a trend of increased CD45+ inflammatory cells at 36 and 72 hours after CCl_4 (Fig. 5E), there was a nearly 3-fold increase in the absolute number of liver infiltrating neutrophils at 36 hours in the AMD3100 treated group (Fig. 5F, 15×10^5 vs. 5×10^5 cells/g). Similarly, FACS analysis revealed an increase in the number of hematopoietic stem cells found in the liver at 36 hours, which was still present, yet not significant at 72 hours (Fig. 5G).

Discussion

Chemokines play a critical role in the progression of liver disease through modulation of hepatic immune cell infiltration and liver parenchymal cell activity [1]. Despite the high levels of CXCL12 expression within the liver, its function is still largely unknown. Previous reports have demonstrated a potential protective role for CXCL12 during injury and regeneration through expansion of hepatic progenitor and oval cells [27-29] and we have shown that it can activate hepatic stellate cells [17].

Here we show that in a murine model of fibrosis, there is an increase in CXCL12 and CXCR4 and that inhibition of this pathway with AMD3100 leads to increased fibrosis and hepatic inflammation. While CXCR4 regulation clearly occurs at the mRNA and protein levels, despite an increase in CXCL12 protein expression there is no change in the transcript levels of any of the murine splice variants indicating that it is not transcriptionally regulated as has been previously reported [29, 30].

We utilized AMD3100, a CXCR4 small molecule inhibitor to modulate the CXCL12/CXCR4 axis during liver injury. As AMD3100 has a very short half-life we used sub-cutaneous osmotic pumps to allow for continual infusion of AMD3100 [31]. In mice receiving AMD3100 there was an increase in the degree of fibrosis, stellate cell activation, and the number of circulating and hepatic inflammatory cells with a specific increase in neutrophils. While CXCL12 promotes stellate cell activation during liver injury treatment with AMD3100 augmented α-SMA expression suggestive of increased stellate cell activity.

Multiple factors converge on stellate cell activation including chemokines, growth factors, and direct cell-cell contact. While inhibition of the CXCL12/CXCR4 axis can mitigate stellate cells activation this effect may have been offset by the increased intrahepatic inflammation and stellate cell activation through a CXCR4-independent mechanism. AMD3100 has allosteric agonist function through CXCR7 [32], which stellate cells express, however, there is no change in activation with AMD3100 treatment in stellate cells with knock down of CXCR7, precluding a role through CXCR7 (data not shown).

In models of myocardial infarction (MI) continuous administration of AMD3100 augments injury, while a single dose, post-MI, promotes egress of bone marrow endothelial progenitor cells, increased myocardial vascularization and better outcomes than controls [13, 14]. As continuous AMD3100 delivery similarly promoted fibrosis in our models, we hypothesized that once weekly delivery of AMD3100 during the course of chronic CCl_4-induced injury would be protective. AMD3100 however had no effect on the extent of fibrosis or inflammation and may be due to the minimal role of ischemic injury in the chronic CCl_4 model. Consequently, these treatments may be beneficial during liver transplantation, where ischemia/reperfusion induced injury is a major sources hepatocyte damage and early organ failure [33, 34].

We next investigated a possible role of AMD3100 as a therapy for acute hepatic injury. Despite the increased survival of rats treated with G-CSF and AMD3100 [24], AMD3100 mono-therapy after acute CCl_4 injury did not reduce the extent of hepatic injury measured by ALT, AST, and necrosis. In fact, similar to our previous results, there was a trend of

worsened injury and increased liver inflammatory cells. Interestingly, at 36 hours post-injury, there was a 3-fold increase in neutrophils, known to be injurious and a 2-fold increase in hematopoietic stem cells, known to be protective. As AMD3100 led to an increase in cell populations with opposing roles, the neutrophilic predominance may have offset any potential beneficial effects of the hematopoietic stem cells.

In all our models, AMD3100 led to an increase in hepatic inflammation. AMD3100 promotes CXCR4 expressing inflammatory cell egress and simultaneously inhibits their recruitment to sites of injury, potentially altering the composition of infiltrating cells and the hepatic response to injury. Furthermore, AMD3100 is now known to preferentially release neutrophils from the lungs, while inhibiting their return to the bone marrow for removal [35], potentially explaining the specific increase of intrahepatic neutrophils seen in mice treated with AMD3100. Interestingly, increased intrahepatic inflammation secondary to AMD3100 alone did not induce any injury response. Only together with CCl_4 treatment did the increased inflammatory cell populations lead to overall worse injury.

In conclusion, treatment with AMD3100 in models of hepatic injury and fibrosis consistently worsened the extent of inflammation and injury. Together our data confirms that inhibition of the CXCR4/CXCL12 axis worsens liver disease by altering the intrahepatic inflammatory response and is not a viable therapeutic target for patients with liver fibrosis.

Acknowledgments

The authors would like to thank Dr. Feng Hong and Hsini Chou for their technical support. This work was supported by NIH grants DK-6047402, DK-071745, and R56DK-092128 (M.B.B.) and DK-090986 (Y.S.).

References

1. Saiman Y, Friedman SL. The role of chemokines in acute liver injury. Front Physiol. 2012; 3:213. [PubMed: 22723782]
2. Seki E, De Minicis S, Gwak G, et al. CCR1 and CCR5 promote hepatic fibrosis in mice. The Journal of Clinical Investigatin. 2009; 119:1858–70.
3. Ajuebor MN, Hogaboam CM, Le T, Swain MG. C-C chemokine ligand 2/monocyte chemoattractant protein-1 directly inhibits NKT cell IL-4 production and is hepatoprotective in T cell-mediated hepatitis in the mouse. Journal of immunology. May 15.2003 170:5252–9.
4. Seki E, de Minicis S, Inokuchi S, et al. CCR2 promotes hepatic fibrosis in mice. Hepatology. Jul. 2009 50:185–97. [PubMed: 19441102]
5. Bonacchi A, Petrai I, Defranco RM, et al. The chemokine CCL21 modulates lymphocyte recruitment and fibrosis in chronic hepatitis C. Gastroenterology. Oct.2003 125:1060–76. [PubMed: 14517790]
6. Zeremski M, Dimova R, Brown Q, Jacobson IM, Markatou M, Talal AH. Peripheral CXCR3-associated chemokines as biomarkers of fibrosis in chronic hepatitis C virus infection. J Infect Dis. Dec 1.2009 200:1774–80. [PubMed: 19848607]
7. Zhang W, Fei Y, Gao J, Liu B, Zhang F. The role of CXCR3 in the induction of primary biliary cirrhosis. Clin Dev Immunol. 2011; 2011:564062. [PubMed: 21647407]
8. Mehrad B, Burdick MD, Zisman DA, Keane MP, Belperio JA, Strieter RM. Circulating peripheral blood fibrocytes in human fibrotic interstitial lung disease. Biochem Biophys Res Commun. Feb 2.2007 353:104–8. [PubMed: 17174272]

9. Harb R, Xie G, Lutzko C, et al. Bone marrow progenitor cells repair rat hepatic sinusoidal endothelial cells after liver injury. Gastroenterology. Aug.2009 137:704–12. [PubMed: 19447108]
10. Hashmi A, Hakim W, Kruglov E, et al. Adenosine inhibits cytosolic calcium signals and chemotaxis in hepatic stellate cells. Am J Physiol Gastrointest Liver Physiol. 2007; 292:G395–G401. [PubMed: 17053161]
11. McCandless EE, Piccio L, Woerner BM, et al. Pathological expression of CXCL12 at the blood-brain barrier correlates with severity of multiple sclerosis. Am J Pathol. Mar.2008 172:799–808. [PubMed: 18276777]
12. Dotan I, Werner L, Vigodman S, et al. CXCL12 is a constitutive and inflammatory chemokine in the intestinal immune system. Inflamm Bowel Dis. Apr.2010 16:583–92. [PubMed: 19774645]
13. Dai S, Yuan F, Mu J, et al. Chronic AMD3100 antagonism of SDF-1alpha-CXCR4 exacerbates cardiac dysfunction and remodeling after myocardial infarction. J Mol Cell Cardiol. Oct.2010 49:587–97. [PubMed: 20655922]
14. Jujo K, Hamada H, Iwakura A, et al. CXCR4 blockade augments bone marrow progenitor cell recruitment to the neovasculature and reduces mortality after myocardial infarction. Proceedings of the National Academy of Sciences of the United States of America. Jun 15.2010 107:11008–13. [PubMed: 20534467]
15. Jantunen E, Lemoli RM. Preemptive use of plerixafor in difficult-to-mobilize patients: an emerging concept. Transfusion. Apr.2012 52:906–14. [PubMed: 21981351]
16. Wald O, Pappo O, Safadi R, Dagan-Berger M, Beider K. Involvement of the CXCL12/CXCR4 pathway in the advanced liver disearse that is associated with hepatitis C virus or hepatitis B virus. Eur J Immunol. 2004; 34:1164–74. [PubMed: 15048728]
17. Hong F, Tuyama A, Lee T, et al. Hepatic Stellate Cells Express Functional CXCR4: Role in Stromal Cell-Derived Factor 1a mediated Stellate Cell Activation. Hepatology. 2009; 49:2055–67. [PubMed: 19434726]
18. Sawitza I, Kordes C, Reister S, Haussinger D. The niche of stellate cells within rat liver. Hepatology. Nov.2009 50:1617–24. [PubMed: 19725107]
19. Wintermeyer P, Cheng CW, Gehring S, et al. Invariant natural killer T cells suppress the neutrophil inflammatory response in a mouse model of cholestatic liver damage. Gastroenterology. Mar.2009 136:1048–59. [PubMed: 19056387]
20. Novobrantseva TI, Majeau GR, Amatucci A, et al. Attenuated liver fibrosis in the absence of B cells. The Journal of clinical investigation. Nov.2005 115:3072–82. [PubMed: 16276416]
21. Karlmark KR, Weiskirchen R, Zimmermann HW, et al. Hepatic recruitment of the inflammatory Gr1+ monocyte subset upon liver injury promotes hepatic fibrosis. Hepatology. Jul.2009 50:261–74. [PubMed: 19554540]
22. Connolly MK, Bedrosian AS, Mallen-St Clair J, et al. In liver fibrosis, dendritic cells govern hepatic inflammation in mice via TNF-alpha. The Journal of clinical investigation. Nov.2009 119:3213–25. [PubMed: 19855130]
23. Takami T, Terai S, Sakaida I. Stem cell therapy in chronic liver disease. Curr Opin Gastroenterol. May.2012 28:203–8. [PubMed: 22395569]
24. Mark AL, Sun Z, Warren DS, et al. Stem cell mobilization is life saving in an animal model of acute liver failure. Ann Surg. Oct.2010 252:591–6. [PubMed: 20881764]
25. Broxmeyer HE, Orschell CM, Clapp DW, et al. Rapid mobilization of murine and human hematopoietic stem and progenitor cells with AMD3100, a CXCR4 antagonist. J Exp Med. Apr 18.2005 201:1307–18. [PubMed: 15837815]
26. Stroncek DF, Clay ME, Herr G, et al. The kinetics of G-CSF mobilization of CD34+ cells in healthy people. Transfus Med. Mar.1997 7:19–24. [PubMed: 9089980]
27. Zheng D, Oh SH, Jung Y, Petersen BE. Oval cell response in 2-acetylaminofluorene/partial hepatectomy rat is attenuated by short interfering RNA targeted to stromal cell-derived factor-1. Am J Pathol. Dec.2006 169:2066–74. [PubMed: 17148669]
28. Mavier P, Martin N, Couchie D, Preaux AM, Laperche Y, Zafrani ES. Expression of stromal cell-derived factor-1 and of its receptor CXCR4 in liver regeneration from oval cells in rat. Am J Pathol. Dec.2004 165:1969–77. [PubMed: 15579440]

29. Tsuchiya A, Imai M, Kamimura H, et al. Increased Susceptibility to Severe Chronic Liver Damage in CXCR4 Conditional Knock-Out Mice. Dig Dis Sci. Jun 5.2012

30. Migliaccio AR, Martelli F, Verrucci M, et al. Altered SDF-1/CXCR4 axis in patients with primary myelofibrosis and in the Gata1 low mouse model of the disease. Experimental hematology. Feb. 2008 36:158–71. [PubMed: 18206727]

31. De Clercq E, Yamamoto N, Pauwels R, et al. Highly potent and selective inhibition of human immunodeficiency virus by the bicyclam derivative JM3100. Antimicrob Agents Chemother. Apr. 1994 38:668–74. [PubMed: 7913308]

32. Kalatskaya I, Berchiche YA, Gravel S, Limberg BJ, Rosenbaum JS, Heveker N. AMD3100 is a CXCR7 ligand with allosteric agonist properties. Molecular pharmacology. May.2009 75:1240–7. [PubMed: 19255243]

33. Martinez-Mier G, Toledo-Pereyra LH, McDuffie JE, Warner RL, Ward PA. Neutrophil depletion and chemokine response after liver ischemia and reperfusion. J Invest Surg. Mar-Apr;2001 14:99–107. [PubMed: 11396626]

34. Zwacka RM, Zhang Y, Halldorson J, Schlossberg H, Dudus L, Engelhardt JF. CD4(+) T-lymphocytes mediate ischemia/reperfusion-induced inflammatory responses in mouse liver. The Journal of clinical investigation. Jul 15.1997 100:279–89. [PubMed: 9218504]

35. Devi S, Wang Y, Chew WK, et al. Neutrophil mobilization via plerixafor-mediated CXCR4 inhibition arises from lung demargination and blockade of neutrophil homing to the bone marrow. J Exp Med. Oct 21.2013 210:2321–36. [PubMed: 24081949]

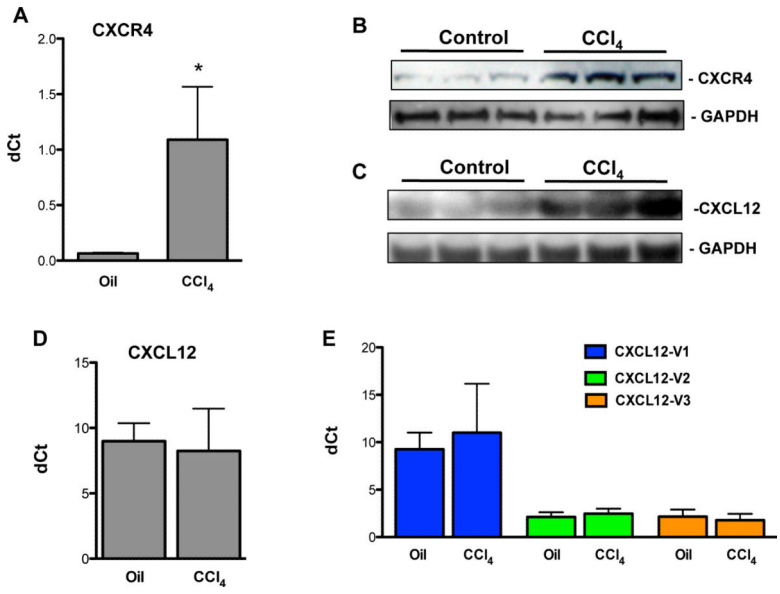

Figure 1. Increased CXCL12 and CXCR4 expression in the chronic CCl_4 model of liver fibrosis

Increased hepatic CXCR4 and CXCL12 expression in mice with CCl_4 induced liver fibrosis by quantitative RT-PCR (A) for CXCR4 and by Western blot for CXCR4 (B) and CXCL12 (C) demonstrates increased CXCR4 mRNA and CXCR4 and CXCL12 protein expression. No changes are seen in CXCL12 mRNA total (D) or splice variants (E) suggesting post-transcriptional regulation. *P<.05.

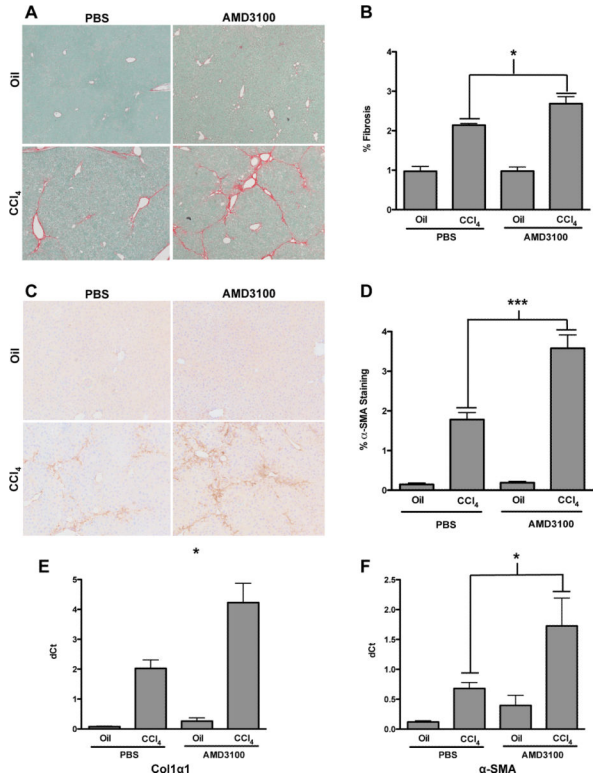

Figure 2. Inhibition of the CXCR4/CXCL12 chemokine axis with continuous infusion of AMD3100 in the chronic CCl_4 model of liver fibrosis promotes hepatic fibrosis

Mice received 4 weeks of CCl_4 with continuous infusion of AMD3100 or PBS by osmotic pumps. Increased fibrosis is seen in AMD3100 treated mice by Sirius red (A) and α-SMA (C) staining. Morphometric analysis was used to quantify the area of Sirius red (B) and α-SMA (D). Quantitative RT-CR further demonstrated an increase in collagen 1α1 (E) and α-SMA (F) transcript levels. Representative images shown, n=6, **P*<.05.

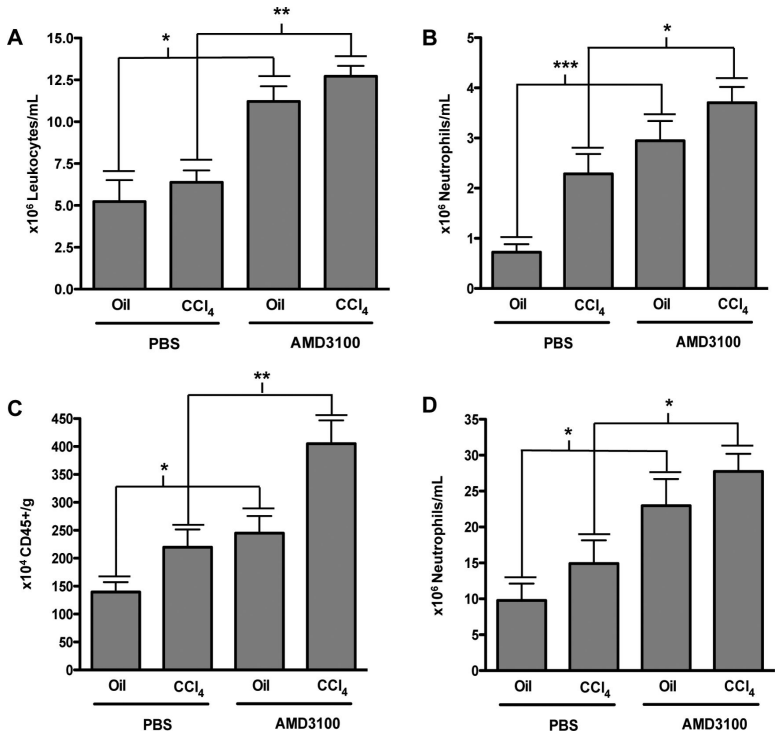

Figure 3. Inhibition of the CXCR4/CXCL12 chemokine axis with continuous infusion of AMD3100 in the chronic CCl_4 model of liver fibrosis promotes liver inflammation

FACS analysis of circulating leukocytes showed that AMD3100 increased circulating inflammatory cells in both oil and CCl_4 treated mice (A), with a specific increase in neutrophil populations (B). Additionally, isolated liver infiltrating inflammatory cells showed an increase in the total number of CD45-positive cells/gram of liver tissue (C) with a similar increase in the absolute number of neutrophils (D) in mice receiving AMD3100 both in oil and CCl_4 treated mice. n=6-12, *P<0.05, **P<.01, ***P<.001.

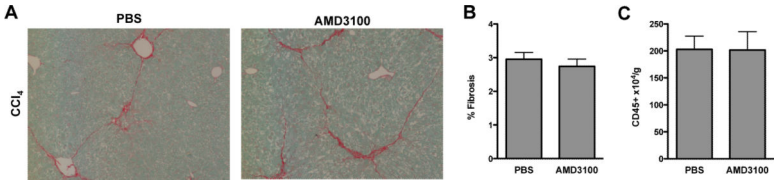

Figure 4. Inhibition of the CXCR4/CXCL12 chemokine axis with once weekly injections of AMD3100 in the chronic CCl_4 model has no effect on hepatic fibrosis and inflammation

Mice received 4 weeks of CCl_4 with once weekly injections of AMD3100. Administration of AMD3100 did not lead to any differences in the degree of fibrosis by Sirius red staining (A) quantified by morphometric analysis (B) or hepatic inflammation (C). Representative images shown, n=5.

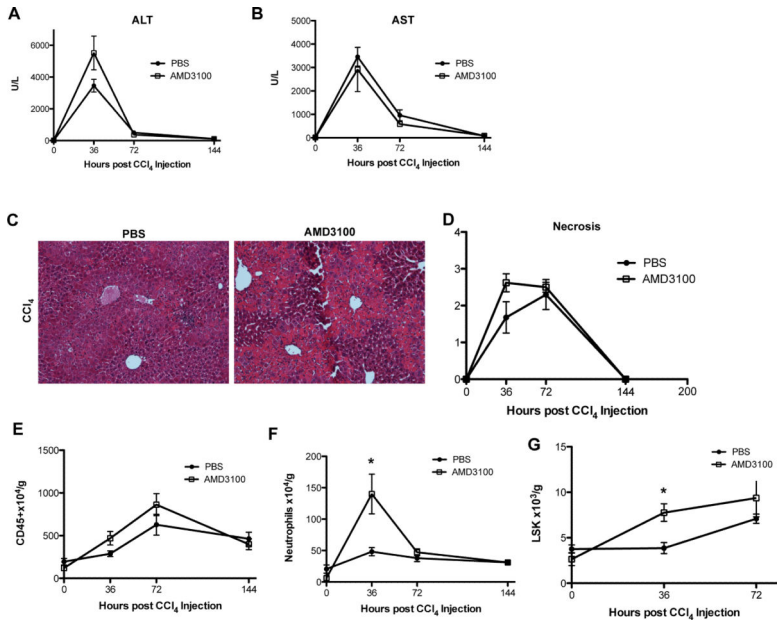

Figure 5. Inhibition of the CXCR4/CXCL12 chemokine axis with a single AMD3100 injection in an acute CCl_4 model does not prevent injury and demonstrates a trend of increased hepatic inflammation

Mice received a single injection of CCl_4 followed by AMD3100 12 hours later and were sacrificed between 36 and 144 hours after the CCl_4 injection. Serum ALT (A) and AST (B) levels showed no significant changes between AMD3100 and control treated groups. In mice treated with AMD3100 H&E images (C) and histological scoring for necrosis (D) showed a trend of increased necrosis at 36 hours, but not at any other time points. FACS analysis of intrahepatic leukocytes similarly showed a trend of increased inflammatory cells (E), with a nearly 3-fold increase of neutrophils at 36, but not 72 hours (F). FACS analysis for hematopoietic stem cells defined as CD45+, lineage negative, Sca-1 +, c-Kit + cells (LSK) showed a significant increase in the absolute number of LSK cells at 36 hours post-CCl_4 injection in mice treated with AMD3100 (G). Representative images shown, n=3-6, **P*<.05.

Table 1

Quantitative RT-PCR Primer Sequences.

Primer Name	Primer Sequence (5'----3')
GAPDH-Forward	CAATGACCCCTTCATTGACC
GAPDH-Reverse	GATCTCGCTCCTGGAAGATG
α-SMA-Forward	TCCTCCCTGGAGAAGAGCTAC
α-SMA-Reverse	TATGGTGGTTTCGTGGATGC
Collagen 1α1-Forward	GTCCCTGAAGTCAGCTGCATA
Collagen 1α1-Reverse	TGGGACAGTCCAGTTCTTCAT
CXCL12-Forward	GCTCTGCATCAGTGACGGTA
CXCL12-Reverse	AGATGCTTGACGTTGGCTCT
CXCL12-V1-Forward	CAACAGACAAGTGTGCATTGACCCG
CXCL12-V1-Reverse	ATGTCAGCCTTCCTCGGGGGT
CXCL12-V2-Forward	ACAGACAAGTGTGCATTGACCCGA
CXCL12-V2-Reverse	ACCTCTCACATCTTGAGCCTCTTGT
CXCL12-V3-Forward	TAGTTCCCCGCTTCCTGCCGATG
CXCL12-V3-Reverse	CCCGAAGAGGGGAGGAGCGAGTT